



Study of a high power density sodium polysulfide/bromine energy storage cell

S.H. GE, B.L. YI* and H.M. ZHANG

Fuel Cell R&D Center, Dalian Institute of Chemical Physics, Chinese Academy of Sciences, Dalian 116023, China

(*author for correspondence, fax: +86-411-4379097, e-mail: blyi@dicp.ac.cn)

Received 19 August 2002; accepted in revised form 8 September 2003

Key words: bromine, cation exchange membrane, energy storage, nickel catalyst, sodium polysulfide

Abstract

Nickel catalyst supported on carbon was made by reduction of nickelous nitrate with hydrogen at high temperature. Ni/C catalyst characterization was carried out by XRD. It was found that the crystal phase of NiS and NiS₂ appeared in the impregnated catalyst. Ni/C and Pt/C catalysts gave high performance as the positive and negative electrodes of a sodium polysulfide/bromine energy storage cell, respectively. The overpotentials of the positive and negative electrodes were investigated. The effect of the electrocatalyst loading and operating temperature on the charge and discharge performance of the cell was investigated. A power density of up to 0.64 W cm⁻² ($V = 1.07$ V) was obtained in this energy storage cell. A cell potential efficiency of up to 88.2% was obtained when both charge and discharge current densities were 0.1 A cm⁻².

1. Introduction

The sodium polysulfide/bromine energy storage cell is based on regenerative fuel cell (RFC) technology. Two electrolytes flow through the cell on either side of a cation exchange membrane. The cell can work at room temperature. It has high efficiency, long life, low cost and is environmentally benign. It is modular and comparatively easy to site. These features make it suitable for large-scale energy storage applications [1–3].

The sodium polysulfide/bromine cell was first reported by Remick [4]. It was developed largely by the UK company Innogy. Using the sodium polysulfide/bromine cell technology, a 120 MWh, 15 MW energy storage plant is expected to be completed in 2003 [2]. The sodium polysulfide/bromine cell technology could be developed for submarine and ship applications as an alternative to the lead-acid battery [5].

Most of the electrodes for the polysulfide redox system are based on metallic sulfide [4, 6–9], carbon composition [10–12] and novel metals [13–15]. Only a modest current density of 10–20 mA cm⁻² at less than 50 mV overpotential was obtained for catalytic electrode surface layers of cobalt and MoS₂ [7]. To improve the electrochemical reaction area, reticulated copper sulfide or nickel sulfide for use as an electrocatalytic material of the polysulfide redox system was reported [9]. When operated at a current density of 40 mA cm⁻², the overpotential was 100 and 30 mV on charging and discharging the cell, respectively [9]. A carbon based electrode also showed modest performance. For the reduction of sulfur at 40 mA cm⁻² the overpotential was 40–75 mV [11]. Elemental sulfur may be formed

during the oxidation of polysulfide ions and the deposited sulfur has a considerable effect on the electrode performance [13–15]. The electrodes for the Br₂/Br⁻ redox couple are mainly based on carbon [16, 17] and platinum [18]. The Br₂/Br⁻ electrode reaction is a version of a chemical–electrochemical (C–E) reaction [19]. The chemical reaction has little effect on the electrode kinetics at very slow homogeneous reaction rates, but has a more drastic effect on the electrode kinetics at faster homogeneous reaction rates [19].

2. Experimental

2.1. Electrode preparation and characterization

Ni/C catalyst for the negative electrode was made by reduction of nickelous nitrate with hydrogen at high temperature. Carbon powder (Vulcan XC-72, Cabot Corp.) was mixed with nickelous nitrate. The weight ratio of Ni to carbon was 1:1. The mixture was dried at 353 K. Then H₂ (flow of 200 cm³ min⁻¹) was fed to the dried mixture and heated at a rate of 2 K min⁻¹, to a final temperature of 773 K. After maintaining the temperature at 773 K for 30 min, it was cooled to room temperature in a H₂ atmosphere.

The negative electrode was prepared as follows: (i) Ni/C catalyst was added to ethanol and treated with ultrasonic agitation for 30 min; (ii) the prepared Ni/C in 50 wt.% ink and Nafion in 50 wt.% solution were mixed with ultrasonic agitation for 20 min; (iii) polyarylonitrile graphite felt was boiled in 1.0 mol l⁻¹ sodium hydroxide solution, rinsed and dried; (iv) the mixture of

the nickel-dispersed carbon powder and Nafion solution was impregnated in the pretreated polyarylonitrile graphite felt and then dried in an oven at 393 K for 30 min under nitrogen atmosphere.

The preparation procedure of the positive electrode was the same as for the negative electrode. The mixture of Pt/C (10 wt.% Pt on XC-72 carbon powder) and Nafion solution was impregnated in the polyarylonitrile graphite felt and then dried.

The impregnated Ni/C catalyst was prepared by heating Ni/C in Na_2S_4 solution at 353 K for 6 h, rinsing in boiling water, boiling in NaOH solution, rinsing in boiling water and drying.

X-ray diffraction (XRD) was performed on a Rijaku D/MAX2400 diffractometer equipped with Cu $K\alpha$ radiation operated at 40 kV and 100 mA. The scan speed was 4° min^{-1} and the scan step was 0.02° .

2.2. Membrane pretreatment

A Nafion membrane was pretreated by boiling in $1 \text{ mol l}^{-1} \text{ H}_2\text{O}_2$ solution, rinsing in boiling water, boiling in 0.5 mol l^{-1} sulfuric acid solution, rinsing in boiling water, boiling in 1.0 mol l^{-1} sodium hydroxide solution and finally rinsing in boiling water.

2.3. Test station and cell configuration

Figure 1 is a schematic diagram showing the principles of the sodium polysulfide/bromine energy storage cell. During charging or discharging the cell, the electrolytes are pumped through two separate chambers of the cell and then flow into the storage tanks.

Figure 2 shows the cell configuration with reference electrode. The negative and positive electrodes were on two sides of Nafion membrane (Du Pont). The reference electrode consisted of a Pt/C catalyst layer and a diffusion layer near the working electrode. The polar plates were waterproof and carved parallel grooves served as flow channels. The frames, gaskets, tie-ins and pipelines were all made of polytetrafluoroethylene. Humidified hydrogen was fed to the reference electrode.

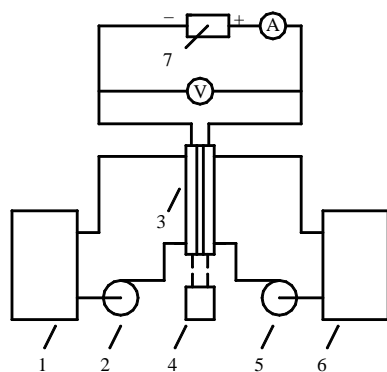


Fig. 1. Schematic diagram of cell test station: (1) negative storage tank; (2, 5) pump; (3) cell; (4) temperature controller; (6) positive storage tank; (7) power supply or load.

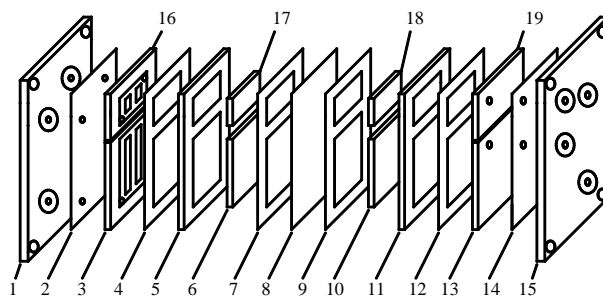


Fig. 2. The structure of cell with reference electrode: (1, 15) end plate; (2, 4, 7, 9, 12, 14) gasket; (3) negative electrode plate; (5, 11) frame; (6) negative electrode; (8) cation exchange membrane; (10) positive electrode; (13) positive electrode plate; (16, 19) reference electrode plate; (17, 18) reference electrode.

Some tests were carried out using a cell without a reference electrode. Its configuration was similar to that with the reference electrode. The difference between these two cells is that electrode area of the usual cell (5 cm^2) was slightly larger than that of the cell with a reference electrode (2 cm^2).

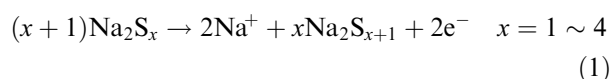
The negative and positive storage tanks were filled with nitrogen gas to negate the influence of oxygen. Unless otherwise mentioned, the operating conditions were as follows:

- The initial negative electrolyte was $2.0 \text{ mol l}^{-1} \text{ Na}_2\text{S}_2$ solution.
- The initial positive electrolyte was $1.0 \text{ mol l}^{-1} \text{ Br}_2$ dissolved in $2.0 \text{ mol l}^{-1} \text{ NaBr}$ solution.
- The flow rates of two electrolytes were about $30 \text{ cm}^3 \text{ min}^{-1}$.

3. Results and discussion

3.1. The principles of the sodium polysulfide/bromine energy storage cell

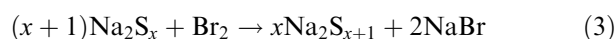
When the sodium polysulfide/bromine energy storage cell is discharging, the sulfide and lower polysulfide compounds are oxidized to corresponding higher polysulfide compounds on the surface of the negative electrode. The simplified electrochemical reaction on the negative electrode is



Positive ions of sodium pass through the cation selective membrane from the negative to the positive side. Bromine is reduced to bromide ions:



The overall chemical reaction is as follows:



The chemical reactions produce an open circuit voltage of about 1.5 V, depending on the concentration and composition of the electrolytes. When the cell is charging, Equation 3 goes from right to left and Na^+ passes through the membrane from the positive to the negative side. The negative and positive electrodes are inert and act only as electron transfer surfaces.

3.2. Catalyst characterization

Figure 3 shows the XRD patterns of fresh and impregnated Ni/C catalysts. In the fresh catalyst, only the Ni crystal phase was identified. The three crystal phases clearly identified were Ni, NiS_2 and NiS after it was impregnated with Na_2S_4 solution. The redox reaction on the negative side of the cell is complex. The catalytic mechanism of Ni in the electrochemical reactions is not yet understood completely and it is difficult to measure the state of Ni *in situ* conditions. The use of sulfided sintered nickel foil as negative electrode has been reported [4]. It may be deduced from XRD results that part of the Ni can be converted to NiS_x in the reaction conditions. Ni and NiS_x may all play important roles in the charging and discharging processes.

3.3. The potential of electrodes

Figures 4 and 5 show the effect of catalyst loading on cell performance and electrode potential when discharging and charging the cell, respectively. The cation exchange membrane was Nafion-115. Nickel loadings on the negative electrode were 10 and 20 mg cm^{-2} . Platinum loadings on the positive electrode were 0.3 and 0.6 mg cm^{-2} . The catalytic activity of polyarylonitrile graphite felt with no catalyst loading is moderate while

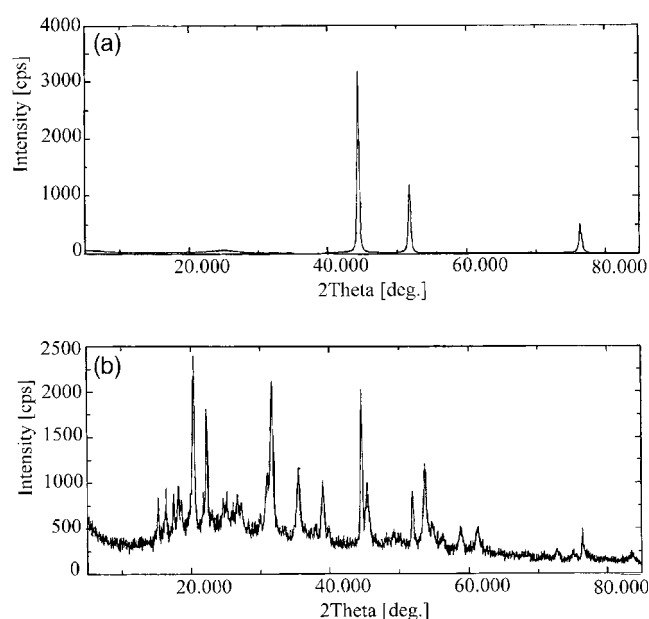


Fig. 3. The XRD patterns of fresh and impregnated Ni/C catalysts: (a) fresh; (b) impregnated.

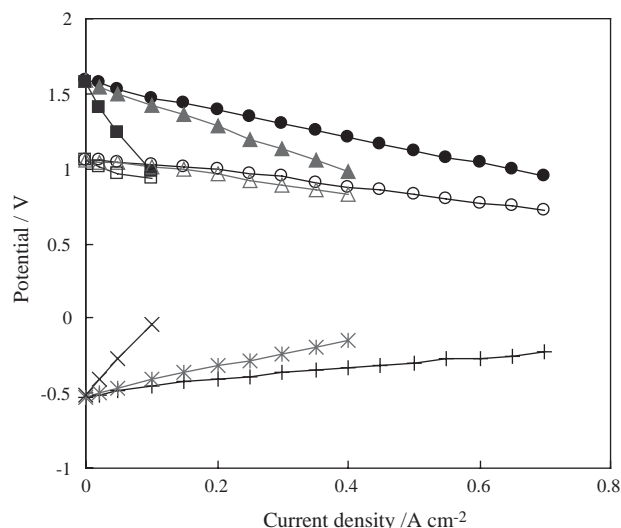


Fig. 4. Potentials of cell and electrode vs current density plots when discharging the cell: (●) cell, (○) positive electrode, (+) negative electrode, $w_{\text{cat,n}} = 20 \text{ mg cm}^{-2}$, $w_{\text{cat,p}} = 0.6 \text{ mg cm}^{-2}$; (▲) cell, (△) positive electrode, (*) negative electrode, $w_{\text{cat,n}} = 10 \text{ mg cm}^{-2}$, $w_{\text{cat,p}} = 0.3 \text{ mg cm}^{-2}$; (■) cell, (□) positive electrode, (×) negative electrode, $w_{\text{cat,n}} = 0 \text{ mg cm}^{-2}$, $w_{\text{cat,p}} = 0 \text{ mg cm}^{-2}$.

discharging. Its catalytic activity is very low while charging. The activity of the negative electrode increases remarkably when Ni/C is used as catalyst. The activity of the positive electrode also increases remarkably when Pt/C is used as catalyst. The overpotentials of the negative and positive electrodes decrease with increasing catalyst loading. Though the performance of the positive electrode with 0.3 mg cm^{-2} platinum loading is slightly lower than that with 0.6 mg cm^{-2} platinum loading, the activity of the electrode with 0.3 mg cm^{-2} platinum loading gives high cell performance. When the cell is discharged at 0.4 A cm^{-2} , the overpotentials of the negative electrode with 10 mg cm^{-2} nickel loading

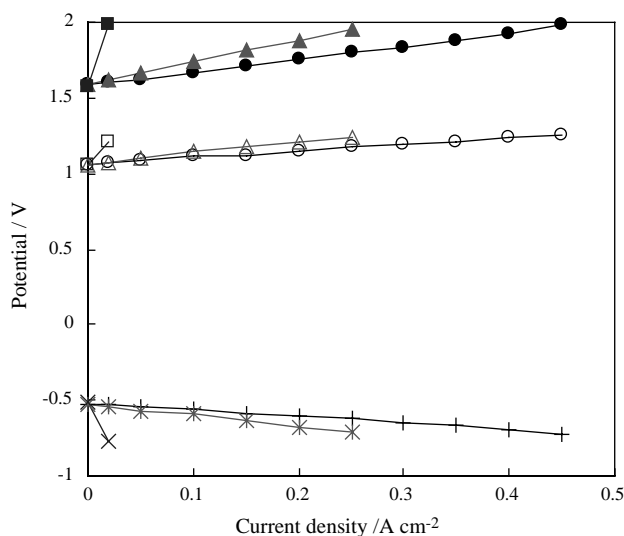


Fig. 5. Potentials of cell and electrode vs current density plots when charging the cell. Symbols are the same as for Figure 4.

and the positive electrode with 0.3 mg cm^{-2} platinum loading are 0.23 and 0.37 V, respectively.

It is important to find an effective way of making an extra-low loading platinum electrode with high performance for the sodium polysulfide/bromine cell. The preparation method of an extra-low loading platinum electrode with high platinum utilization and performance will be reported in a future paper.

3.4. Effect of operating conditions on the cell performance

Figure 6 shows the effect of temperature on the charge and discharge performances of the sodium polysulfide/bromine cell. The nickel loading on the negative electrode is 20.0 mg cm^{-2} . The platinum loading on the positive electrode is 0.6 mg cm^{-2} . The cell performance increases with increasing temperature, both in the charging and discharging processes. A charge current density of up to 0.5 A cm^{-2} (at $V = 1.97 \text{ V}$) and discharge current density of up to 0.6 A cm^{-2} (at $V = 1.07 \text{ V}$) were obtained in this novel energy storage cell at 368 K. A power density of up to 0.74 W cm^{-2} (at $i = 0.8 \text{ A cm}^{-2}$, $V = 0.93 \text{ V}$) was obtained at 368 K.

There can be several reasons for improved cell performance with increasing temperature. Firstly, the catalyst activity increases. Secondly, ohmic overpotential in the membrane decreases with increasing temperature. Diffusion inside the membrane for Na^+ depends on the water content and temperature [20]. Thirdly, the mass transport overpotentials in the electrodes decrease with increasing temperature. Szykarczuk reported that polysulfide could be oxidized to elemental sulfur at a platinum electrode. The formation of a layer of sulfur film could significantly reduce the rate of electrochemical reaction [15]. The dissolution rates of sulfur in sulfide and lower polysulfide compounds increase with increasing temperature. An elevated temperature causes the

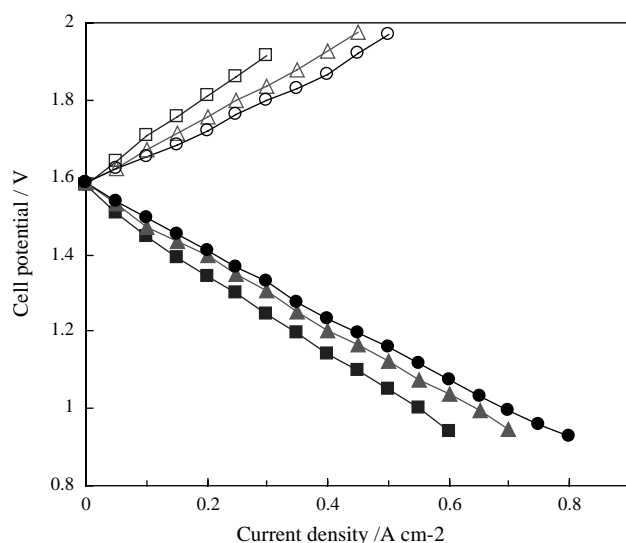


Fig. 6. Cell potential vs current density plots for the cell with different temperature: (●) discharge, (○) charge, 368 K; (▲) discharge, (△) charge, 353 K; (■) discharge, (□) charge, 323 K.

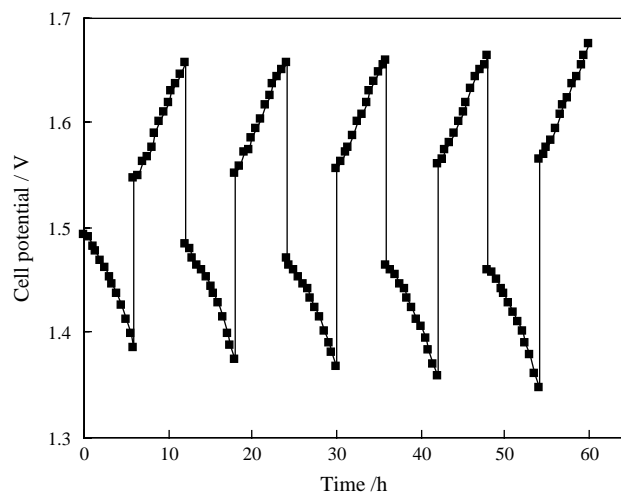


Fig. 7. Cell potential vs time plots in the charge/discharge cycles.

sulfur layer to be dissolved more quickly and results in high discharge performance of the sodium polysulfide/bromine energy storage cell.

3.5. Cell performance over a few cycles

Figure 7 shows cell potential vs time plots for five cycles of the cell. The nickel loading on the negative electrode was 20.0 mg cm^{-2} . The platinum loading on the positive electrode was 0.6 mg cm^{-2} . The initial volumes of the negative and positive electrolyte solutions were 100 cm^3 and operating temperature was 368 K. Fresh solutions were used. The cell was operated over five cycles (60, 6 h discharge and 6 h charge). The charge and discharge current densities were kept constant at 0.1 A cm^{-2} . In the 6 h discharge of the first cycle, the cell voltage decreases from 1.49 to 1.39 V, in the 6 h charge of the first cycle, the cell voltage increases from 1.55 to 1.66 V. It can be seen that after five cycles the discharge and charge performances decreased slightly. A cell potential efficiency of up to 88.2% was obtained in these five cycles.

It is not possible for the Nafion membrane to give 100% permselectivity. During cycling of the cell, sulfide ions and polysulfide ions may diffuse from the negative to the positive side, and bromine and bromide may diffuse from the positive to the negative side. The slight diffusion of unwanted species across the membrane may result in a decrease in current efficiency and cell performance.

4. Conclusions

High power density and efficiency were obtained for the sodium polysulfide/bromine energy storage cell. Ni/C and Pt/C catalysts gave high performance as the positive and negative electrodes, respectively. The activity of the positive electrode with 0.3 mg cm^{-2} platinum loading is sufficiently high to obtain excellent cell performance. A

charge current density of up to 0.5 A cm^{-2} (at $V = 1.97 \text{ V}$) and a discharge current density of up to 0.6 A cm^{-2} (at $V = 1.07 \text{ V}$) were obtained.

High operating temperature improves the cell performance both in the charge and discharge processes. The oxidative reaction in the negative side is complex. Ni can react with polysulfide ions to form NiS and NiS₂. Elevated temperature causes the sulfur layer to dissolve quickly and results in high discharge performance.

The discharge and charge performances decrease slightly after five cycles. The small amount of diffusion of unwanted species across the membrane may result in a decrease in current efficiency and cell performance.

Acknowledgements

Financial support for this project from the National Postdoctoral Science Foundation of China is gratefully acknowledged.

References

1. A.C.R. Price, 'Renewable Energy Storage', (IMechE Seminar Publication, 2000) vol. 7 p. 11.
2. [Anon], *TCE* **736** (2002) 16.
3. A. Price, S. Bartley, S. Male and G. Cooley, *Power Eng. J.* **13** (1999) 122.
4. R.J. Remick and P.G.P. Ang, US Patent 4485154 (1984).
5. J.B. Lakeman, P. Barnes, W. Cranstone, S. Male, I. Whyte, G.E. Cooley and P. Mitchell, *Warship* **99** (1999) 1.
6. G. Hodes and J. Manassen, *J. Electrochem. Soc.* **127** (1980) 544.
7. P.M. Lessner, F.R. McLarnon, J. Winnick and E.J. Cairns, *J. Appl. Electrochem.* **22** (1992) 927.
8. P. Lessner, J. Winnick, F.R. McLarnon and E.J. Cairns, *J. Electrochem. Soc.* **133** (1986) 2517.
9. W.R.I. Cranstone, G.E. Cooley, S.E. Male and J.D. Cox, WO Patent 0016420 (2000).
10. R. Zito, WO Patent 9409526 (1994).
11. T.J. Calver, S.E. Male, P.J. Mitchell and I. Whyte, GB Patent 2337150 (1999).
12. D.G. Clark, M.C. Turpin, I. Whyte and G.E. Cooley, WO Patent 0015576 (2000).
13. A.J. Ahern, L.D. Burke, D.P. Casey and P.J. Morrissey, *Proc. – Electrochem. Soc.* **23** (2001) 174.
14. M. Behm and D. Simonsson, *J. Appl. Electrochem.* **27** (1997) 507.
15. J. Szynekarczuk, P.G. Komorowski and J.C. Donini, *Electrochim. Acta* **39** (1994) 2285.
16. R.F. Savinell and S.D. Fritts, *J. Power Sources* **22** (1988) 423.
17. K.J. Cathro, K. Cedzynska and D.C. Constable, *J. Power Sources* **19** (1987) 337.
18. B.E. Conway, Y. Phillips and S.Y. Qian, *J. Chem. Soc., Faraday Trans.* **91** (1995) 283.
19. P.K. Adanuvor, R.E. White and S.E. Lorimer, *J. Electrochem. Soc.* **134** (1987), 1450.
20. A.L. Rollet, J.P. Simonin and P. Turq, *Phys. Chem. Chem. Phys.* **2** (2000) 1029.